

# DeepSensor: Deep Learning Testing Framework Based on Neuron Sensitivity

Haibo Jin, Ruoxi Chen, Haibin Zheng, Jinyin Chen, Zhenguang Liu, Qi Xuan, Yue Yu, Yao Cheng

**Abstract**—Despite their impressive capabilities and outstanding performance, deep neural networks (DNNs) have captured increasing public concern about their security problems, due to their frequently occurred erroneous behaviors. Therefore, it is necessary to conduct a systematical testing for DNNs before they are deployed to real-world applications. Existing testing methods have provided fine-grained metrics based on neuron coverage and proposed various approaches to improve such metrics. However, it has been gradually realized that a higher neuron coverage does *not* necessarily represent better capabilities in identifying defects. To bridge the gap, we design a novel white-box testing framework for DNNs based on the concept of neuron sensitivity, namely DeepSensor. DeepSensor is motivated by our observation that neurons whose activation values change dramatically due to minor perturbations are more likely related to incorrect corner cases due to potential defects. By maximizing the number of sensitive neurons via particle swarm optimization, DeepSensor can effectively trigger more diverse corner cases due to different reasons. Extensive experiments implemented on three datasets and seven models demonstrate the superiority of DeepSensor. Compared to the state-of-the-art testing approaches, by generating the same number of testing examples, DeepSensor can find more test errors than baselines ( $\sim \times 1.2$ ), especially on polluted data ( $\sim \times 5$ ) and incompletely-trained DNNs ( $\sim \times 1.3$ ). Besides, the generated testing examples can reach higher neuron coverage ( $\sim \times 2$ ), and increase the model's  $l_2$ -norm robustness bound by up to 0.2 via retraining. We further analyze the impact of the neuron sensitivity and the number of sensitive neurons on the quality of generated testing examples and interpret the effectiveness of generated testing examples via visualization for better understanding.

**Index Terms**—Deep learning, testing, robustness, white-box testing.

## I. INTRODUCTION

This research was supported by the National Natural Science Foundation of China (No. 62072406), the Natural Science Foundation of Zhejiang Province (No. LY19F020025), and the Key Laboratory of the Public Security Ministry Open Project in 2020 (No. 2020DSJSYS001). (Corresponding author: Jinyin Chen and Haibin Zheng.)

H. Jin, R. Chen and H. Zheng are with the College of Information Engineering, Zhejiang University of Technology, Hangzhou, 310023, China. (email: 2112003035@zjut.edu.cn, 2112003149@zjut.edu.cn, haibinzheng320@gmail.com)

J. Chen and X. Qi are with the Institute of Cyberspace Security and the College of Information Engineering, Zhejiang University of Technology, Hangzhou, 310023, China. (email: chenjinyin@zjut.edu.cn, xuanqi@zjut.edu.cn)

Z. Liu is with the School of Computer and Information Engineering, Zhejiang Gongshang University, Hangzhou, 310023, China. (email: liuzhengguang2008@gmail.com)

Y. Yue is with the Key Laboratory of Parallel and Distributed Computing, College of Computer, National University of Defense Technology, Changsha, 410000, China. (email: yuyue@nudt.edu.cn)

Y. Cheng is with the Huawei International, Singapore (email: chengyao101@huawei.com)

**D**EEP neural networks (DNNs) have achieved tremendous progress over the last few decades and enjoyed increasing popularity in a variety of applications such as image classification [1], [2], [3], computer vision [4], [5], speech recognition [6], natural language processing [7], [8], [9] and medical diagnosis [10]. Despite their impressive capabilities and outstanding performance, DNNs' security and robustness have raised massive public concern. DNNs often expose unexpected erroneous behaviors, which may finally lead to disastrous consequences especially in safety-critical applications such as autonomous driving [11]. Therefore, it is important to systematically test the DNN models before deploying them to safety and security critical domains. DNN testing aims to explore as many as possible incorrect corner case behaviors in advance so that potential flaws in DNN models can be identified and further fixed.

Extensive efforts have been made to test vulnerabilities of DNNs. White-box DNN testing, which is inspired by the success of code coverage criteria in traditional software testing, was first proposed in DeepXplore [12]. Such testing methods are mainly coverage-criterion guided, which focus on improving neuron coverage in testing example generation via well-established mutation testing. Along this direction, DeepGuage [13], DLFuzz [14] and DeepHunter [15] are developed, further improving the exploratory degree.

However, higher neuron coverage does *not* indicate better defect-finding capability [16]. In the testing phase, existing white-box approaches show good performance in finding adversarial inputs. This is because they use the gradient of the neuron output to generate testing examples, similar to the generation of adversarial examples. However, they may fail to find defects due to polluted training data and incompletely-trained models (i.e., underfitting or overfitting models) in the training phase. Polluted data and benign data jointly participate in the training to tune the model parameters, i.e., the neuron weights and bias values. In this case, testing examples guided by neuron coverage may not be able to trigger unexpected erroneous behaviors.

To address the problem, we reconsider the potential defects from the angle of neurons behaviors. Specifically, we believe that neurons that change their activation values dramatically due to minor input perturbations, i.e., neurons that are sensitive to input perturbations, are prone to trigger erroneous corner cases, regardless of defects from testing or training phase.

We conduct an experiment to verify our assumption. In order to quantitatively measure the activation value changes due to input perturbations, we propose the concept of *neuron sensitivity* (which will be defined later in Eq. 1). Neurons

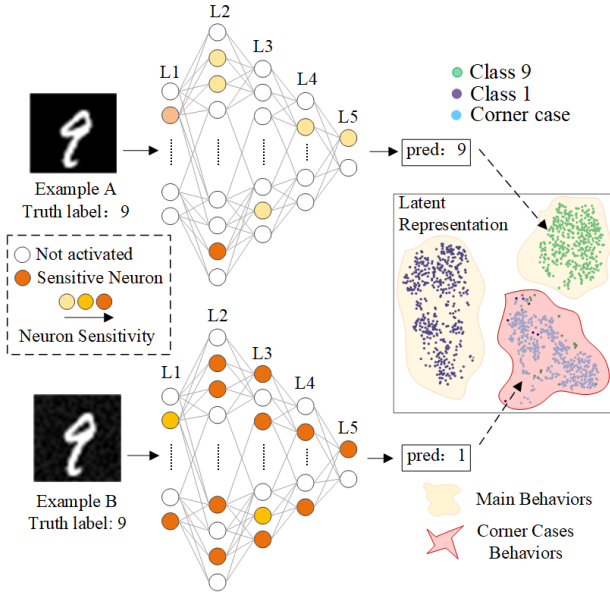


Fig. 1. The relationship between sensitive neurons and corner case behaviors on LeNet-5 of MNIST.

with neuron sensitivity values larger than a threshold (e.g., 0.5 in this experiment) are considered as sensitive neurons. The experiment is using the same well-trained LeNet-5 [17] of MNIST [18] on 500 pairs of examples, i.e., a benign example from class “9” and one of its corner case versions. Fig. 1 shows one of such example pairs. We observe that the number of sensitive neurons that are activated by the corner case example B is much more than that of the benign example A. For better understanding, we visualize the latent representations of examples from class “1”, class “9” and the corner cases using t-SNE [19]. We can see that they form three different clusters, and the examples in the corner case cluster are generally activate more sensitive neurons than that from the other clusters.

From this experiment, we gain the insight that an input example that activates more sensitive neurons in the model may expose more unexpected corner case behaviors of that model. Therefore, instead of being guided by the neuron coverage metrics, in this paper, we generate testing examples leveraging the fundamental neuron behaviors in DNN. We develop a white-box testing framework DeepSensor which generates testing examples by maximizing the number of sensitive neurons via particle swarm optimization (PSO) [20], which finds the optimal solution through the collaboration and information sharing between individuals in the group. We demonstrate that DeepSensor not only performs better in finding test errors but also achieves higher neuron coverage than the state-of-the-art baselines though DeepSensor is not designed specially to improve the neuron coverage.

Our contributions are summarized as follows.

- We propose the definition of neuron sensitivity, which measures activation value changes due to input perturbations. We take the first exploration towards the relationship between sensitive neurons and potential defects in the model, and gain the insight that sensitive neurons are closely related to the model’s incorrect corner case

behaviors due to various potential defects.

- We develop a novel white-box DNN testing framework DeepSensor. By maximizing the number of sensitive neurons via PSO, DeepSensor can generate testing examples that trigger more unexpected corner case behaviors due to various potential defects.
- Compared to the state-of-the-art testing approaches, by generating the same number of testing examples, DeepSensor can find more test errors than baselines ( $\sim \times 1.2$ ), especially on polluted data ( $\sim \times 5$ ) and incompletely-trained DNNs ( $\sim \times 1.3$ ). Besides, generated testing examples can reach higher neuron coverage ( $\sim \times 2$ ), and increase the model’s  $l_2$ -norm robustness bound by up to 0.2 via retraining.

## II. RELATED WORK

### A. Testing Methods for DNNs

Generally speaking, testing methods can be divided into black-box and white-box methods.

**Black-box methods.** Black-box testing methods achieve testing without observing the internal behaviors of models. Wicker et al. [21] used scale invariant feature transform (SIFT) to extract key points and generate testing examples, whose effectiveness is demonstrated on adversarial attacks. Ma et al. [22] proposed DeepMutation, which defines a set of source level or model level mutation operators for quality evaluation of test data. Wang et al. [23] proposed a lightweight robustness metric based on first-order loss, and use it for generating testing examples for improving model robustness.

**White-box methods.** Different from black-box methods, white-box ones reach the objective from the inside perspective of model. Pei et al. [12] proposed DeepXplore and introduced neuron coverage to systematically measure the parts of the DNN exercised by the testing examples. However, it is difficult to measure all neuron behaviors with one single metric. Ma et al. [13] put forward a set of multi-granularity test standards for DNNs at a more fine-grained level, including neuron coverage (NC), strong neuron activation coverage (SNAC),  $k$ -multisection neuron coverage (TMNC), top- $k$  neuron patterns (TKNP), top- $k$  neuron coverage (TKNC) and neuron boundary coverage (NBC). Guo et al. [14] proposed DLFuzz based on differential fuzzing, with larger neuron coverage and more generated adversarial inputs. Besides, Odena et al. [24] developed coverage-guided fuzzing methods TensorFuzz, for generating random mutations of the input. TensorFuzz can find numerical errors in DNNs. Xie et al. [15] proposed DeepHunter, which generates mutation examples under the guidance of multiple coverage feedback using mutation based optimization. It realizes further detection of potential corner cases. Lee et al. [25] proposed ADAPT that can adaptively determine neuron-selection strategies during testing.

### B. Neuron-based Approaches

Neurons, which are the fundamental element in DNNs, have been analyzed to detect and defense against adversarial attacks. The success of these works motivates us to explore the sensitivity of neuron activation in assisting DNN testing.

**Adversarial detection.** Ma et al. [26] observes the neuron activation value changes under various adversarial attacks. Two indicators, i.e., value invariants (VI) and the provenance invariants (PI), are proposed for adversarial detection. Shan et al. [27] first injected trapdoors and honeypot into the data, which attacker's optimization algorithm will fall into. Adversarial attacks can hence be detected by comparing the neuron activation signatures of an input to those of the trapdoor.

**Adversarial defense.** Bai et al. [28] put forward channel-wise activation suppressing (CAS), which suppresses redundant activation from being activated by adversarial perturbations during training. Zhang et al. [29] explained the adversarial robustness from the perspective of neuron sensitivity, measured by changes of neuron behaviors against benign and adversarial examples. They further used sensitive neuron stabilizing (SNS) to improve model robustness.

### C. Certified Robustness

Certified robustness provides guarantees of robustness to norm bounded attacks. Szegedy et al. [30] calculated the global Lipschitz constants of each layer and used their product to explain the robustness of DNNs. Gehr et al. [31] proposed an end-to-end analyzer  $AI^2$ , which can automatically verify the security of DNNs. Moreover, Weng et al. [32] proposed robustness measurement called cross Lipschitz extreme value for network robustness (CLEVER). The minimum size of perturbations for adversarial examples to fool models is estimated by extreme value theory as well. CLEVER is the first attack-independent robustness metric that can be applied to any DNN, which we use to evaluate the robustness improvement in our experiment.

### D. Optimization Algorithms

Here we introduce several commonly-used optimization algorithms.

Inspired by the foraging behavior of some ant species, Dorigo et al. [33] proposed ant colony optimization (CAO) to stimulate the process of ant foraging. It is easy to combine with other methods, but takes high computation cost. Genetic algorithm (GA) [34] is motivated by the evolutionary laws in nature, which searches for best solution via three genetic operators, including selection, crossover and mutation. Its robustness and scalability has been demonstrated in many applications, with low efficiency and complex parameters left to be solved. Particle swarm optimization (PSO) is an evolutionary computation approach developed by Kennedy et al. [20]. In PSO, each particle can record the historical optimal position, and the group can be optimized through the information sharing between the particles. It converges fast with fewer parameters, but easy to stuck at local optima. PSO is chosen in our method due to its excellent optimization performance. Besides, we search for the global approximate optimal solution by changing initialization strategy, which will be discussed in experimental evaluation.

## III. METHODOLOGY

### A. Preliminaries

Given a DNN with  $l$  layers and let  $N_i = \{n_1, n_2, \dots\}$  be a set of neurons of  $i$ -th layer. Let  $X = \{x_1, x_2, \dots\}$  denote a set of testing examples and  $\Delta x$  is the perturbation. We introduce a function  $\varphi_i(x, n)$  that measures the output of a neuron  $n \in N_i$ , where  $x \in X$  represents a testing example.

**Definition 1 (Neuron sensitivity)** Given a neuron  $n$ , the neuron sensitivity is defined as:

$$NS_n(x, \Delta x) = \frac{\varphi_n(x + \Delta x) - \varphi_n(x)}{\|\Delta x\|_2} \quad (1)$$

where  $\|\cdot\|_2$  represents  $l_2$ -norm and  $NS_n(x, \Delta x)$  denotes the neuron sensitivity of neuron  $n$  feed with testing input  $x$  and perturbation  $\Delta x$ .

**Definition 2 (Sensitive neuron)** Given a neuron  $n$  and an input  $x \in X$ , and a threshold  $\lambda$ . If  $NS_n(x, \Delta x) > \lambda$ , it is considered as sensitive neuron. We maximize the number of these neurons in the process of generating testing examples, for further triggering diverse corner cases.

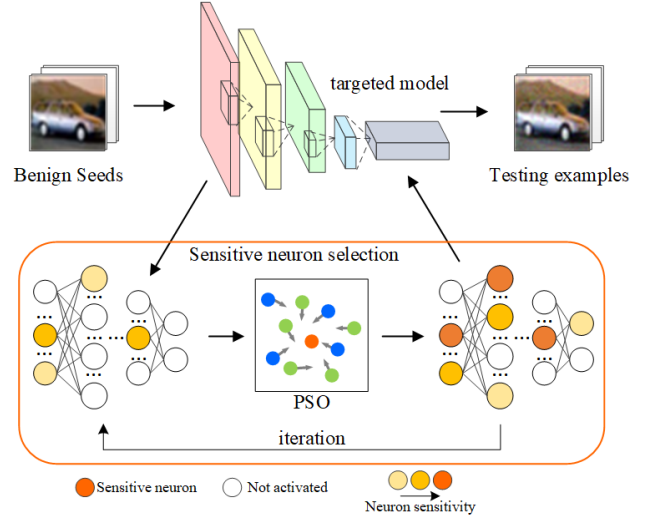


Fig. 2. The overview of DeepSensor.

### B. Overview of DeepSensor

The overview of DeepSensor is shown in Fig. 2, which mainly includes two steps, i.e., sensitive neuron selection and testing example generation.

More specifically, benign seeds are first fed into the targeted model for sensitive neuron selection. The number of the sensitive neurons are used as optimization objective to be maximized. Global maximum can be reached during iterations of PSO, where the search direction is updated according to the value of fitness function. Finally, testing examples are generated for triggering more corner cases. The pseudo-code of DeepSensor is presented in Algorithm 1.

### C. The Fitness Function

Fitness function is the main reference basis in the PSO optimization, which is also crucial to generating testing examples. We need to maximize the number of sensitive neurons

**Algorithm 1** Generation of testing examples

**Input:** Benign seeds  $X = \{x_1, x_2, \dots\}$ . Fitness threshold  $\epsilon$ . Population size  $NUM$ . The maximum iteration  $G_k$ .

**Output:** Generated examples  $X^* = \{x_1^*, x_2^*, \dots\}$ .

```

1:  $X^* = \{\emptyset\}$ 
2: for  $x$  in  $X$  do
3:    $p_{best}, g_{best} = \text{InitializeSwarm}(x)$ 
4:   for current iteration  $g \leq G_k$  do
5:      $\text{Fitness}(x^*) = \text{CalculateFitness}(x)$ 
6:     for  $i = 0 : NUM$  do
7:       if  $\text{Fitness}(x^*) > p_{best}$  then
8:          $p_{best} = \text{Fitness}(x^*)$ 
9:         if  $\text{Fitness}(x^*) > g_{best}$  then
10:           $g_{best} = \text{Fitness}(x^*)$ 
11:        end if
12:      end if
13:       $\text{CalculateSpeed}(x^*)$ 
14:       $\text{UpdatePosition}(x^*)$ 
15:    end for
16:     $g = g + 1$ 
17:    if  $g_{best} > \epsilon$  then
18:      break
19:    end if
20:  end for
21:  The best solution  $x^*$  is found
22:   $X^* \leftarrow X^* \cup x^*$ 
23: end for

```

during the iteration of generating examples. Hence, the fitness function is designed as the following equation shows.

$$\text{Fitness} = \frac{\sum_{i \in l} \{n \mid \forall x \in X : NS_n(x^*, n) > \lambda\}}{\sum_{i \in l} Num_i} \quad (2)$$

where  $x^* = x + \Delta x$  denotes the generated testing example and  $Num_i$  denotes the total number of neurons in  $i$ -th layer.  $\sum$  means sum function and the fitness function calculates the percentage of sensitive neurons.

In the initialization phase, the value of fitness function is 0 because  $x$  is equal to  $x^*$ . The number of sensitive neurons is supposed to increase significantly during the iterations. As shown in Line 17 in Algorithm 1, the current iteration will end if the value of the fitness function is larger than a threshold  $\epsilon$ .

#### D. Testing Example Generation via PSO

To start the PSO, we first need to initialize the particle swarms randomly. Here, the initial position matrix  $x_p$  of the input particle  $x \in X$  is set to the RGB values of pixels in each seed example, and the change of the pixel value in  $x$  is taken as the velocity matrix  $v$ .

During iterations, the fitness value of a single particle can be calculated according to Eq. 2. Then we compare the current value with the previous best values of particle swarms, and update the previous optimal position  $p_{best}$  of each particle, as well as the global optimal position  $g_{best}$ .

Next, the speed  $v$  and position  $x_p$  of the particle swarm will be updated as shown in the equations below. Non-negative inertia weight is adopted in the update process to avoid the problem of local optimum. The updating formula of velocity consists of three parts, i.e., the momentum part, the individual and the group part. The momentum part is responsible for velocity maintenance, and the individual and group part guarantee the approach towards  $p_{best}$  and  $g_{best}$ , respectively.

$$\omega^g = (\omega_{initial} - \omega_{end})(G_k - g)/G_k + \omega_{end} \quad (3)$$

$$v_i = \omega^g \times v_i + c_1 \times rand(\cdot) \times (p_{best} - x_p) + c_2 \times rand(\cdot) \times (g_{best} - x_p) \quad (4)$$

$$x_p = x_p + v \quad (5)$$

where  $\omega^g$ ,  $\omega_{initial}$  and  $\omega_{end}$  denote the current, initial and final weight vector, respectively.  $g$  represents the number of current iteration and  $G_k$  is the maximum iteration.  $c_1$  and  $c_2$  are learning factors, usually are set to 2. The former is responsible for individual learning while the latter for group learning.  $rand(\cdot)$  represents the function that generates random number in the interval of [0,1].

Steps above will repeat until the value of fitness reaches threshold  $\epsilon$  or  $g$  reaches the maximum iteration  $G_k$ . The approximate optimal solution is used as the final testing example.

It is generally believed that the global version of the particle swarm algorithm converges quickly, but easily falls into a local optimum. To avoid the problem, we randomly assign the initial location of each swarm before iterations. In this way, in the process of updating the particle position, global optimal can be reached with a higher probability.

## IV. EXPERIMENT

### A. Setup

**Platform.** CPU is Intel XEON 6240 2.6GHz x 18C, GPU is Tesla V100 32GiB, the Memory is DDR4-RECC 2666 16GiB, the operating system is Ubuntu 16.04, the programming language is Python 3.6, the deep learning framework is Tensorflow-gpu-1.10.0.

**Datasets.** MNIST [18] is a handwritten digit dataset, which contains 70,000 28×28 gray-scale images. 50,000 examples are used for training, 10,000 for testing. Each is marked with numbers from 0 to 9. CIFAR-10 [35] dataset consists of 60,000 32×32 RGB-color images, which are divided into ten classes equally. ImageNet [36] is a large set of conventional images for classification. It includes 1.4 million training data and 50,000 test data from 1,000 classes.

**DNNs.** Various models are adopted in our experiments. On MNIST, we adopt three LeNet family models [17] (i.e., the LeNet-1, LeNet-4, LeNet-5), abbreviated as “LN-1”, “LN-4” and “LN-5”. ResNet-20 (Res-20) [1] and VGG16 [37] are used for CIFAR-10. For ImageNet, experiments are implemented on two pre-trained models MobileNet (MNet) [38] and ResNet-50 (Res-50) [1]. The classification accuracy and model configurations are detailed in Table I. Please note that “acc” gained

here is calculated on the benign examples we need in the experiment, not on all examples from the whole dataset.

TABLE I  
WELL-TRAINED MODELS USED IN EXPERIMENTS.

Datasets	Models	#Parameters	#Layers	#Neurons	acc
MNIST	LeNet-1	7,206	7	52	98.40%
	LeNet-4	69,362	8	148	98.90%
	LeNet-5	107,786	9	268	98.90%
CIFAR-10	ResNet-20	273,066	71	1,882	91.70%
	VGG16	33,663,070	17	12,426	90.80%
ImageNet	MobileNet	4,231,976	87	38,904	87.10%
	ResNet-50	25,583,592	176	94,059	92.90%

**Baselines.** We compare DeepSensor with three state-of-the-art testing methods for fair comparison, including DeepXplore [12], DeepHunter [15] and DLFuzz [14]. DeepXplore is conducted under the guidance of NC and “blackout” is used. We instantiated DLFuzz with the strategy that performs best, with  $neuron\_to\_cover\_num = 10$  and  $k=4$ . DeepHunter is based on SNAC, based on which can find more corner cases. Neuron boundary of SNAC is calculated by 1,000 examples. The number of iterations of all testing methods is set to 20.

**Metrics.** ① Classification accuracy:  $acc = \frac{n_{true}}{n_{benign}}$ , where  $n_{true}$  is the number of clean examples correctly classified by the targeted model and  $n_{benign}$  denotes the total number of benign images.

② Attack success rate:  $ASR = \frac{n_{adv}}{n_{total}}$ , where  $n_{adv}$  denotes the number of examples misclassified by the targeted model after attacks.  $n_{total}$  represents the number of total number of examples.

③ Robustness measurement CLEVER [32]: CLEVER computes the lowest robust boundary  $L_{p,x_0}^j$  through sampling a set of points  $x^j$  around an input  $x_0$  and takes the maximum value of  $\|\Delta g(x_0)\|_p$ , which is calculated as:  $L_{p,x_0}^j = \max_{x \in \mathbb{B}_p(x_0, R)} \|\Delta g(x_0)\|_p$ , where  $g(x_0) = f_c(x_0) = f_j(x_0)$  and  $c, j$  are two different classes.

④ Coverage-based criteria: NC, KMNC, NBC, SNAC, TKNC, BKNC. The detail definitions of them can be found in [15].

⑤ Perturbation  $l_2$ -distance:  $\rho = \|x^* - x\|_2$ , where  $x$  and  $x^*$  are benign and its corresponding testing example respectively, and  $\|\cdot\|_2$  represents  $l_2$ -norm.

### B. Effectiveness in Finding Defects

Here we conduct experiment to evaluate the default finding capabilities of DeepSensor, including errors due to adversarial inputs, polluted data and incompletely-trained DNNs. The parameters in DeepSensor are set as,  $c_1 = 2$ ,  $c_2 = 2$ ,  $\omega_{initial} = 0.4$ ,  $\omega_{end} = 0.9$ ,  $\lambda = 0.5$ ,  $\epsilon = 1$ , and  $G_k = 10$ .

1) *On adversarial inputs:* We run DeepSensor and baselines using 1,000 benign seeds for 20 iterations. We count the total number of test errors found (#Test errors), the total number of error categories found by different methods (#Error categories), and the number of error categories found per benign seed (#Average categories). The experimental results are shown in Table II.

Generally, DeepSensor is superior to testing baselines. DeepSensor successfully triggers more diverse errors, i.e., av-

TABLE II  
EFFECTIVENESS IN FINDING ADVERSARIAL INPUTS.

Datasets	Models	Testing Strategies	#Test errors	#Error categories	#Average categories
MNIST	LeNet-1	DeepXplore	17,528	2,667	2.667
		DLFuzz	17,490	1,682	1.682
		DeepHunter	18,124	2,682	2.682
		DeepSensor	<b>18,747</b>	<b>3,168</b>	<b>3.168</b>
	LeNet-4	DeepXplore	18,474	2,379	2.379
		DLFuzz	16,809	1,473	1.473
		DeepHunter	18,420	2,489	2.489
		DeepSensor	<b>18,771</b>	<b>2,868</b>	<b>2.868</b>
	LeNet-5	DeepXplore	18,076	2,224	2.224
		DLFuzz	16,914	1,509	1.509
		DeepHunter	18,323	2,469	2.469
		DeepSensor	<b>18,349</b>	<b>2,906</b>	<b>2.906</b>
CIFAR-10	ResNet-20	DeepXplore	16,723	1,162	1.162
		DLFuzz	15,989	1,336	1.336
		DeepHunter	17,384	1,549	1.549
		DeepSensor	<b>18,025</b>	<b>2,024</b>	<b>2.024</b>
	VGG16	DeepXplore	16,759	1,007	1.007
		DLFuzz	15,567	1,107	1.107
		DeepHunter	17,693	1,680	1.680
		DeepSensor	<b>17,784</b>	<b>1,964</b>	<b>1.964</b>
	MobileNet	DeepXplore	13,974	689	0.689
		DLFuzz	14,046	1,974	1.974
		DeepHunter	15,120	2,287	2.287
		DeepSensor	<b>15,524</b>	<b>2,994</b>	<b>2.994</b>
ImageNet	ResNet-50	DeepXplore	11,894	673	0.673
		DLFuzz	12,271	1,281	1.281
		DeepHunter	12,985	1,590	1.590
		DeepSensor	<b>13,042</b>	<b>2,010</b>	<b>2.010</b>

TABLE III  
EFFECTIVENESS IN FINDING ERRORS DUE TO POLLUTED DATA.

Models	$\alpha$	#Test errors			
		DeepXplore	DLFuzz	DeepHunter	DeepSensor
LeNet-5	10%	74	204	192	<b>757</b>
	20%	79	164	181	<b>723</b>
	30%	72	172	185	<b>784</b>
VGG16	10%	64	91	101	<b>590</b>
	20%	60	127	92	<b>562</b>
	30%	62	121	147	<b>599</b>
ResNet-50	10%	42	83	64	<b>511</b>
	20%	58	64	101	<b>648</b>
	30%	50	61	77	<b>639</b>

eragely triggers more categories. The reason is that DeepSensor focuses on sensitive neurons, which are directly related to model’s prediction. By random choosing the initial position of particle swarms during iterations, DeepSensor can generate diverse testing examples with a high probability to trigger diverse errors. Specially for larger models, DeepSensor exhibits stable performance in covering error categories (achieving up to 2 times of the baselines), which shows striking contract to DeepXplore’s performance decrease.

TABLE IV  
EFFECTIVENESS IN FINDING TEST ERRORS IN INCOMPLETELY-TRAINED DNNs.

Models	Config.	#Test errors			
		DeepXplore	DLFuzz	DeepHunter	DeepSensor
LeNet-5	underfitting	880	814	891	<b>981</b>
	well-trained	894	845	906	<b>937</b>
	overfitting	837	826	898	<b>979</b>
VGG16	underfitting	813	790	853	<b>949</b>
	well-trained	831	791	858	<b>901</b>
	overfitting	820	808	829	<b>958</b>
ResNet-50	underfitting	513	600	620	<b>796</b>
	well-trained	525	604	627	<b>672</b>
	overfitting	545	580	611	<b>805</b>

TABLE V  
CONFIGURATIONS OF MODELS UNDER THE SETTING OF POLLUTED DATA AND INCOMPLETELY-TRAINED DNNs.

Models	Patch size	Polluted class	#Epoch	Polluted data		Retrained acc			Incompletely-trained DNNs			
				Batch size	#Training data	$\alpha=10\%$	$\alpha=20\%$	$\alpha=30\%$	Config.	#Epoch	Batch size	Retrained acc
LeNet-5	min=1×1, max=6×6	‘1’	10	32	60,000	97.4%	98.3%	97.2%	overfitting	30	32	99.91%
									underfitting	1	512	79.32%
VGG16	min=3×3 max=8×8	‘bird’	80	64	60,000	89.8%	88.9%	89.4%	overfitting	120	64	98.20%
									underfitting	5	64	76.03%
ResNet-50	min=10×10 max=15×15	‘Siberian husky’	80	64	20,000	91.2%	90.7%	90.4%	overfitting	120	64	98.74%
									underfitting	30	64	79.32%

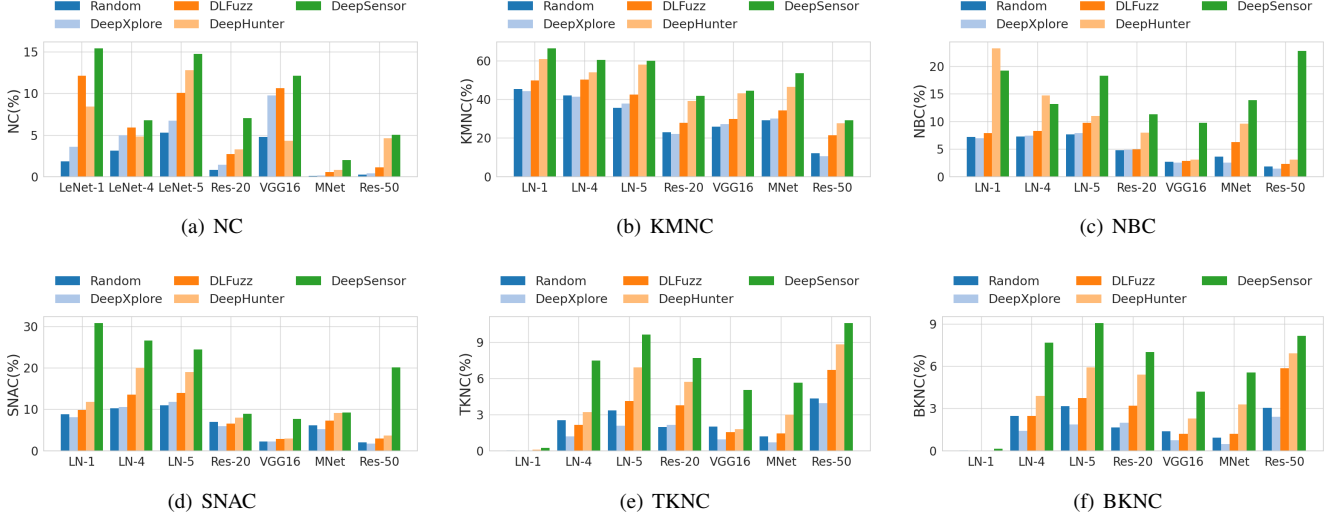


Fig. 3. The improvement of neuron coverage.

2) *On polluted data:* We further investigate the performance of DeepSensor on finding errors due to polluted data. In order to obtain the models trained with polluted data, We retrain the model with manually polluted data by randomly drawing  $\alpha\%$  examples, stamping perturbations of random sizes at random location, and re-labeling them as one of the original classes, i.e., the polluted class. Configuration details can be found in Table V. We generate 1,000 testing examples using DeepSensor and the three baselines. The test examples that trigger the polluted class are counted as test errors. The results are shown in Table III.

As shown in Table III, DeepSensor performs well in finding more errors due to polluted labels, which triggers almost five times errors more than baselines among all datasets and models. One of the reasons could be that the polluted and benign data jointly contribute to the model training. The benign and polluted examples may show similar neuron coverage. However, the features of the polluted data are likely to be captured by the sensitive neurons. By maximizing the number of sensitive neurons, DeepSensor can easily hunt errors left by polluted data.

3) *On incompletely-trained DNNs:* We also conduct exploratory experiments on finding defects due to incompletely-trained DNNs, which have not been studied before. We trained overfitting and underfitting models for LeNet-5, VGG16 and ResNet-50, and generate 1,000 testing examples to test these models. The configurations of model settings are also presented in Table V and the experimental results are shown in Table IV.

According to Table V, DeepSensor finds the most test errors, superior to all three baselines on all models, regardless of overfitting or underfitting ones. Specifically, DeepSensor can generate more effective testing examples that hunt more errors for incompletely-trained models than for well-trained models. On the contrary, three baselines do not show such distinct characteristics in three types of models. We conjecture that the incompletely-trained DNNs may have more sensitive neurons so that DeepSensor can maximizing the number of sensitive neurons more easily, and hence can generate more effective testing examples.

### C. Evaluation in Neuron Coverage Metrics

DeepSensor is not designed to improve the neuron coverage as the baselines do. However, we are still interested in how DeepSensor performs in terms of traditional neuron coverage metrics. We generate 1,000 testing examples from 1,000 benign seeds and calculate the neuron coverage for both. Random strategy, which generates normally distributed noise, is conducted as baselines here as well. The improvement measured by the six neuron coverage metrics are shown in Fig. 3. The testing examples are limited by the  $l_2$  distance to its benign seed. The  $l_2$  distance is limited to 1 on MNIST and CIFAR-10, and 2 on ImageNet. The threshold in NC is set to 0.2 and  $k$  in KMNC is 10,000. For TKNC and BKNC, top-1 neurons are calculated.

We can see from Fig. 3 that the test examples generated by all methods improve these metrics than that of benign seeds.



The improvement by DeepSensor exceeds that of baselines in most cases, up to 2 times on average. Though existing studies show that neuron coverage does not necessarily indicate better defect-finding capability [16], neuron coverage metrics are still important measurement in DNN testing. DeepSensor, which achieves best in finding test errors (see Table II), also demonstrates high values in traditional neuron coverage metrics although it is not guided by neuron coverage. This supports our assumption that the number of sensitive neurons are closely related to the triggering of corner cases and hence DeepSensor may show high values in various neuron coverage metrics.

We also observe that the performance of baseline methods is not consistent in the six metrics. DeepXplore shows higher NC than Random but is inferior to Random on five other metrics. On NBC, DeepHunter outperforms all methods on LeNet-1 and LeNet-4, but is less effective than DLFuzz on NC on these models.

#### D. Adversarial Robustness Improvement

By retraining the model with the generated examples, the robustness of the model can be improved significantly. The robustness improvement highly depends on the quality of the retraining data. We compare the robustness improvement by different testing example generation methods using both empirical measurement ASR and certified robustness metric CLEVER. We retrain the model using 500 benign examples and their 500 corresponding testing examples by DeepSensor and the baseline methods for 20 epochs with batch\_size=32. The benign accuracy is barely affected by the retraining.

1) *On ASR*: We attack the retrained model using the state-of-the-art first-order attack PGD [39].  $\epsilon$  in PGD is set to 0.3 for MNIST and CIFAR-10 and 0.5 for ImageNet. We compare the ASR of the retrained model and the original model. The decrease in ASR is shown in Fig.4(a), the more, the better. Compared with baselines, models retrained with testing examples generated by DeepSensor are more robust against attacks, i.e., more decrease in ASR, which in turn demonstrates the better quality of testing examples generated by DeepSensor.

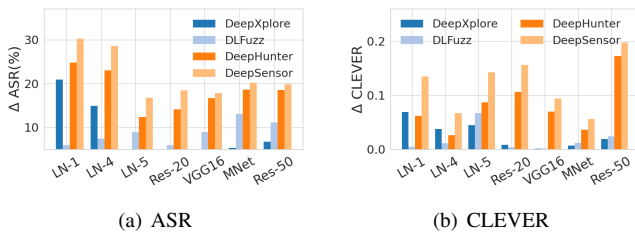


Fig. 4. The change in ASR and CLEVER between original and retrained models.

2) *On CLEVER*: CLEVER is an attack-independent certified robustness metric. We measure the improvement in CLEVER after retraining using testing examples generated by DeepSensor and the baselines. The sampling parameters  $N_b$  and  $N_s$  in CLEVER are set to 500 and 1024, respectively. The increase in CLEVER is shown in Fig.4(b), the larger, the

better. CLEVER scores on retrained models are significantly improved. DeepSensor increases the  $l_2$  norm certified robustness by up to 0.2, better than all baselines.

#### E. Interpretation of Sensitive Neurons

There are two parameters in DeepSensor that control the effect of sensitive neurons, i.e.,  $\lambda$  defining the sensitive neurons and  $\epsilon$  controlling the threshold of sensitive neuron percentage in PSO.

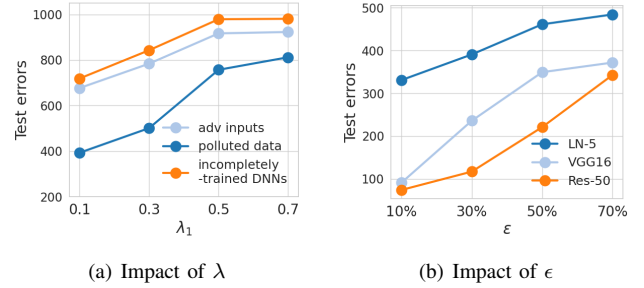


Fig. 5. Impact of neuron sensitivity on DeepSensor.

1)  $\lambda$ :  $\lambda$  defines what neurons are considered as sensitive neurons in DeepSensor, the value of which is crucial to DeepSensor's performance. We investigate the impact of different  $\lambda$  values on DeepSensor's performance in finding test errors, the results of which are shown in Fig. 5(a). We are using 500 testing examples for MNIST LeNet-5 model. Here,  $\alpha$  in polluted data is 10% and overfitting model is used.

With the increase of  $\lambda$ , the number of test errors found by DeepSensor gradually increases and then remains stable after 0.6. A smaller  $\lambda$  means that the neurons DeepSensor focuses on during the optimization are less sensitive. As a consequence, the testing examples generated may not benefit from the "true" sensitive neurons, and it benefits DeepSensor by increasing  $\lambda$ . However, a larger  $\lambda$  means the neurons with larger sensitivity are focused by DeepSensor during the optimization and less sensitive neurons are considered in the process, which hence limit the optimization objective, i.e., maximizing the number of sensitive neurons.

2)  $\epsilon$ :  $\epsilon$  controls the percentage of sensitive neurons in the fitness function used in PSO. According to our assumption, it is more more likely to expose erroneous behaviors with more sensitive neurons activated. This experiment investigates the impact of  $\epsilon$  on DeepSensor using 500 testing examples for finding adversarial inputs, the results of which also supports our assumption.

As shown in Fig. 5(b), the number of test errors found by DeepSensor increases with the increase of the percentage of sensitive neurons. By maximizing the number of sensitive neurons, more corner case behaviors can be triggered by DeepSensor.

#### F. Impact of Initial Position of Swarms in PSO

Here we analyze the effectiveness of random initialization strategy in DeepSensor, which is proposed for avoiding local optimum. We compare random location initialization (i.e., the

initial location of each swarm before iterations is randomly chosen) with the fixed one, on hunted test errors due to adversarial inputs, polluted data and incompletely-trained DNNs. 1,000 testing examples are generated for evaluation. Results on LeNet-5 and ResNet-50 are shown in Fig. 6, where blue and red bars denote the number of test errors found and six neuron coverage improvement by fixed and random strategy, respectively.

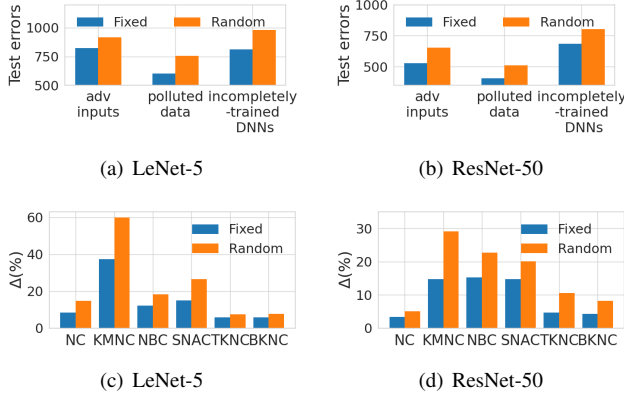


Fig. 6. The impact of random location initialization. The first row represents the impact on finding test errors while the second row represents that on six neuron coverage improvement.

It can be easily observed that hunted test errors of random strategy outperforms that of fixed one on six metrics and both models. This indicates that more sensitive neurons can be found during iterations when particle position is random initialized. As a result, more test errors can be triggered regardless of their causes, as well as global optimal, can be reached with less time to converge. Similar trends can also be found on six neuron coverage metrics. Dramatically change of KMNC is obviously seen, since we increase the number of sensitive neurons directly and indirectly through the threshold, so we achieve more coverage in the initial upper and lower bounds of neurons. In this way, the problem of local optimum can be alleviated.

### G. Visualization

1) *Visualization of t-SNE*: Visualization can help better understand the generated testing examples. Here, we visualize the high-dimensional representation of benign examples and the generated testing examples via t-SNE.

As shown in Fig. 7, we visualize two classes of benign examples (“Class 1” and “Class 2”), and the testing examples generated by DeepHunter and our DeepSensor using “Class 1” examples as seeds. We only visualize the generated examples that are classified as “Class 1” and “Class 2” for a clear demonstration. They are represented in red, orange, green and blue, respectively.

A well-trained model can well distinguish examples from different classes, i.e., clusters of “Class 1” and “Class 2” are separate from each other in all three figures. The testing examples of DeepHunter and DeepSensor form two clusters different from the two benign classes, which means they may trigger corner cases and lead to misclassification. However,

the testing examples generated by DeepHunter considerably overlap with “Class 1”. It means that these examples may not be able to do so, which also explains the experimental results in Table II that DeepHunter triggers less test errors than DeepSensor.

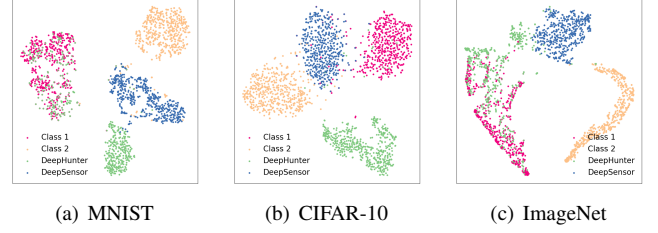


Fig. 7. t-SNE visualizations on LeNet-5 of MNIST, ResNet-20 of CIFAR-10 and ResNet-50 of ImageNet.

2) *Visualization of testing examples*: Testing examples generated by DeepSensor are shown in Fig. 8. The first, middle and last row are from MNIST, CIFAR-10 and ImageNet datasets respectively. Columns 1 and 7 show original images with their labels attached at the bottom of them, while columns 2 and 5 are testing examples with their labels. All perturbations,  $\rho$  for short, are magnified 10 times for better visualization. It can be easily observed that testing examples closely resemble original images, with perturbation nearly imperceptible to human eyes. This well demonstrates the performance of DeepSensor that corner cases could be triggered by small size of perturbations.

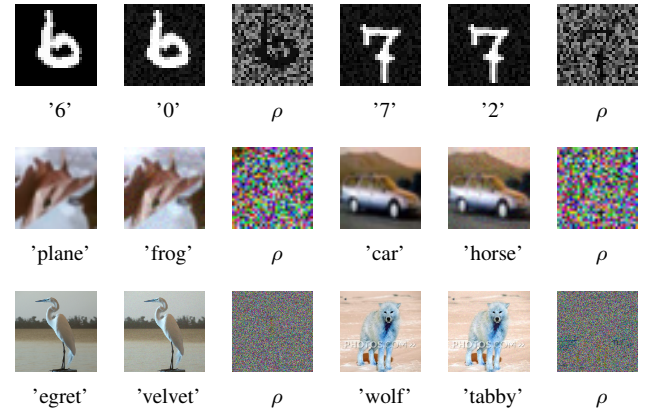


Fig. 8. Testing examples on MNIST, CIFAR-10 and ImageNet datasets generated by DeepSensor.

### H. Time Complexity Comparison

We also evaluate the efficiency of DeepSensor by comparing the time cost of generating 100 testing examples by DeepSensor and the baselines. The results are shown in Table VI. We can see DeepSensor needs less time than baselines to generate the same number of testing examples, especially in larger models with larger input dimensions.

## V. CONCLUSIONS

In this paper, we propose DeepSensor, a novel white-box DNN testing approach that leveraging on the sensitive neurons.



TABLE VI  
COMPARISON OF TIME COMPLEXITY

Datasets	Models	Time/s			
		DeepXplore	DLFuzz	DeepHunter	DeepSensor
MNIST	LeNet-5	222.88	178.61	102.20	<b>101.41</b>
CIFAR-10	VGG16	1242.38	987.46	437.25	<b>411.33</b>
ImageNet	ResNet-50	1454.14	1174.78	624.30	<b>576.64</b>

By maximizing the number of sensitive neurons, DeepSensor can generate testing examples that perform better in various effectiveness and efficiency metrics than the state of the art testing methods.

However, the efficiency of DeepSensor could still be further improved. In the future, we will work towards lower algorithm complexity and deeper exploration in hidden space. Furthermore, we intend to improve DeepSensor so that it distinguish errors due to misclassified natural inputs for more reliable fault-detection capability.

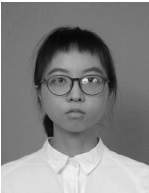
## REFERENCES

- [1] K. He, X. Zhang, S. Ren, and J. Sun, "Deep residual learning for image recognition," in *Proceedings of the IEEE conference on computer vision and pattern recognition*, 2016, pp. 770–778.
- [2] H. Yuan and Y. Y. Tang, "Spectral-spatial shared linear regression for hyperspectral image classification," *IEEE Trans. Cybern.*, vol. 47, no. 4, pp. 934–945, 2017. [Online]. Available: <https://doi.org/10.1109/TCYB.2016.2533430>
- [3] Z. Wen, Z. Hou, and L. Jiao, "Discriminative dictionary learning with two-level low rank and group sparse decomposition for image classification," *IEEE Trans. Cybern.*, vol. 47, no. 11, pp. 3758–3771, 2017. [Online]. Available: <https://doi.org/10.1109/TCYB.2016.2581861>
- [4] Y. Li, Y. Zhang, and Z. Zhu, "Error-tolerant deep learning for remote sensing image scene classification," *IEEE Trans. Cybern.*, vol. 51, no. 4, pp. 1756–1768, 2021. [Online]. Available: <https://doi.org/10.1109/TCYB.2020.2989241>
- [5] M. Sun, Z. Zhou, Q. Hu, Z. Wang, and J. Jiang, "SG-FCN: A motion and memory-based deep learning model for video saliency detection," *IEEE Trans. Cybern.*, vol. 49, no. 8, pp. 2900–2911, 2019. [Online]. Available: <https://doi.org/10.1109/TCYB.2018.2832053>
- [6] W. Xiong, J. Droppo, X. Huang, F. Seide, M. Seltzer, A. Stolcke, D. Yu, and G. Zweig, "Achieving human parity in conversational speech recognition," *arXiv preprint arXiv:1610.05256*, 2016.
- [7] L. Deng and Y. Liu, *Deep learning in natural language processing*. Springer, 2018.
- [8] X. Wang, L. Kou, V. Sugumaran, X. Luo, and H. Zhang, "Emotion correlation mining through deep learning models on natural language text," *IEEE Trans. Cybern.*, vol. 51, no. 9, pp. 4400–4413, 2021. [Online]. Available: <https://doi.org/10.1109/TCYB.2020.2987064>
- [9] X. Li, A. Yuan, and X. Lu, "Vision-to-language tasks based on attributes and attention mechanism," *IEEE Trans. Cybern.*, vol. 51, no. 2, pp. 913–926, 2021. [Online]. Available: <https://doi.org/10.1109/TCYB.2019.2914351>
- [10] M. Liu, J. Zhang, C. Lian, and D. Shen, "Weakly supervised deep learning for brain disease prognosis using MRI and incomplete clinical scores," *IEEE Trans. Cybern.*, vol. 50, no. 7, pp. 3381–3392, 2020. [Online]. Available: <https://doi.org/10.1109/TCYB.2019.2904186>
- [11] F. Lambert, "Understanding the fatal tesla accident on autopilot and the nhtsa probe," *Electrek*, July, vol. 1, 2016.
- [12] K. Pei, Y. Cao, J. Yang, and S. Jana, "Deepxplore: Automated whitebox testing of deep learning systems," in *proceedings of the 26th Symposium on Operating Systems Principles*, 2017, pp. 1–18.
- [13] L. Ma, F. Juefei-Xu, F. Zhang, J. Sun, M. Xue, B. Li, C. Chen, T. Su, L. Li, Y. Liu *et al.*, "Deepgauge: Multi-granularity testing criteria for deep learning systems," in *Proceedings of the 33rd ACM/IEEE International Conference on Automated Software Engineering*, 2018, pp. 120–131.
- [14] J. Guo, Y. Jiang, Y. Zhao, Q. Chen, and J. Sun, "Dlfuzz: Differential fuzzing testing of deep learning systems," in *Proceedings of the 2018 26th ACM Joint Meeting on European Software Engineering Conference and Symposium on the Foundations of Software Engineering*, 2018, pp. 739–743.
- [15] X. Xie, L. Ma, F. Juefei-Xu, M. Xue, H. Chen, Y. Liu, J. Zhao, B. Li, J. Yin, and S. See, "Deephunter: a coverage-guided fuzz testing framework for deep neural networks," in *Proceedings of the 28th ACM SIGSOFT International Symposium on Software Testing and Analysis*, 2019, pp. 146–157.
- [16] Z. Li, X. Ma, C. Xu, and C. Cao, "Structural coverage criteria for neural networks could be misleading," in *2019 IEEE/ACM 41st International Conference on Software Engineering: New Ideas and Emerging Results (ICSE-NIER)*. IEEE, 2019, pp. 89–92.
- [17] Y. LeCun *et al.*, "Lenet-5, convolutional neural networks," URL: <http://yann.lecun.com/exdb/lenet>, vol. 20, no. 5, p. 14, 2015.
- [18] Y. LeCun, L. Bottou, Y. Bengio, and P. Haffner, "Gradient-based learning applied to document recognition," *Proceedings of the IEEE*, vol. 86, no. 11, pp. 2278–2324, 1998.
- [19] L. Van der Maaten and G. Hinton, "Visualizing data using t-sne," *Journal of machine learning research*, vol. 9, no. 11, 2008.
- [20] R. Eberhart and J. Kennedy, "A new optimizer using particle swarm theory," in *MHS'95. Proceedings of the Sixth International Symposium on Micro Machine and Human Science*. Ieee, 1995, pp. 39–43.
- [21] M. Wicker, X. Huang, and M. Kwiatkowska, "Feature-guided black-box safety testing of deep neural networks," in *International Conference on Tools and Algorithms for the Construction and Analysis of Systems*. Springer, 2018, pp. 408–426.
- [22] L. Ma, F. Zhang, J. Sun, M. Xue, B. Li, F. Juefei-Xu, C. Xie, L. Li, Y. Liu, J. Zhao *et al.*, "Deepmutation: Mutation testing of deep learning systems," in *2018 IEEE 29th International Symposium on Software Reliability Engineering (ISSRE)*. IEEE, 2018, pp. 100–111.
- [23] J. Wang, J. Chen, Y. Sun, X. Ma, D. Wang, J. Sun, and P. Cheng, "Robot: Robustness-oriented testing for deep learning systems," in *2021 IEEE/ACM 43rd International Conference on Software Engineering (ICSE)*. IEEE, 2021, pp. 300–311.
- [24] A. Odena, C. Olsson, D. Andersen, and I. Goodfellow, "Tensorfuzz: Debugging neural networks with coverage-guided fuzzing," in *International Conference on Machine Learning*. PMLR, 2019, pp. 4901–4911.
- [25] S. Lee, S. Cha, D. Lee, and H. Oh, "Effective white-box testing of deep neural networks with adaptive neuron-selection strategy," in *Proceedings of the 29th ACM SIGSOFT International Symposium on Software Testing and Analysis*, 2020, pp. 165–176.
- [26] S. Ma and Y. Liu, "Nic: Detecting adversarial samples with neural network invariant checking," in *Proceedings of the 26th Network and Distributed System Security Symposium (NDSS 2019)*, 2019.
- [27] S. Shan, E. Wenger, B. Wang, B. Li, H. Zheng, and B. Y. Zhao, "Gotta catch'em all: Using honeypots to catch adversarial attacks on neural networks," in *Proceedings of the 2020 ACM SIGSAC Conference on Computer and Communications Security*, 2020, pp. 67–83.
- [28] Y. Bai, Y. Zeng, Y. Jiang, S.-T. Xia, X. Ma, and Y. Wang, "Improving adversarial robustness via channel-wise activation suppressing," in *International Conference on Learning Representations*, 2020.
- [29] C. Zhang, A. Liu, X. Liu, Y. Xu, H. Yu, Y. Ma, and T. Li, "Interpreting and improving adversarial robustness of deep neural networks with neuron sensitivity," *IEEE Transactions on Image Processing*, vol. 30, pp. 1291–1304, 2020.
- [30] C. Szegedy, W. Zaremba, I. Sutskever, J. Bruna, D. Erhan, I. Goodfellow, and R. Fergus, "Intriguing properties of neural networks," *arXiv preprint arXiv:1312.6199*, 2013.
- [31] T. Gehrmann, M. Mirman, D. Drachler-Cohen, P. Tsankov, S. Chaudhuri, and M. Vechev, "Ai2: Safety and robustness certification of neural networks with abstract interpretation," in *2018 IEEE Symposium on Security and Privacy (SP)*. IEEE, 2018, pp. 3–18.
- [32] T.-W. Weng, H. Zhang, P.-Y. Chen, J. Yi, D. Su, Y. Gao, C.-J. Hsieh, and L. Daniel, "Evaluating the robustness of neural networks: An extreme value theory approach," *arXiv preprint arXiv:1801.10578*, 2018.
- [33] M. Dorigo, M. Birattari, and T. Stützle, "Ant colony optimization," *IEEE Comput. Intell. Mag.*, vol. 1, no. 4, pp. 28–39, 2006. [Online]. Available: <https://doi.org/10.1109/MCI.2006.329691>
- [34] E. K. Burke and D. B. Varley, "A genetic algorithms tutorial tool for numerical function optimisation," in *Proceedings of the 2nd Annual Conference on Integrating Technology into Computer Science Education, ITICSE 1997, Uppsala, Sweden, 1-5 June, 1997*, L. N. Cassel, M. Daniels, J. E. Miller, and G. Davies, Eds. ACM, 1997, pp. 27–30. [Online]. Available: <https://doi.org/10.1145/268819.268830>
- [35] A. Krizhevsky, G. Hinton *et al.*, "Learning multiple layers of features from tiny images," 2009.
- [36] O. Russakovsky, J. Deng, H. Su, J. Krause, S. Satheesh, S. Ma, Z. Huang, A. Karpathy, A. Khosla, M. Bernstein *et al.*, "Imagenet large scale visual recognition challenge," *International journal of computer vision*, vol. 115, no. 3, pp. 211–252, 2015.

- [37] K. Simonyan and A. Zisserman, "Very deep convolutional networks for large-scale image recognition," *arXiv preprint arXiv:1409.1556*, 2014.
- [38] A. G. Howard, M. Zhu, B. Chen, D. Kalenichenko, W. Wang, T. Weyand, M. Andreetto, and H. Adam, "Mobilenets: Efficient convolutional neural networks for mobile vision applications," *arXiv preprint arXiv:1704.04861*, 2017.
- [39] A. Madry, A. Makelov, L. Schmidt, D. Tsipras, and A. Vladu, "Towards deep learning models resistant to adversarial attacks," in *6th International Conference on Learning Representations, ICLR 2018, Vancouver, BC, Canada, April 30-May 3, 2018*. OpenReview.net, 2018, pp. 1–28.



**Haibo Jin** has been working toward the MS degree in the Institute of Information Engineering, Zhejiang University of Technology, Hangzhou, China. His research interest include artificial intelligence, and adversarial attack and defense.



**Ruoxi Chen** is currently pursuing the masters degree with the Institute of Information Engineering, Zhejiang University of Technology, Hangzhou, China. Her research interest covers deep learning and AI security.



**Haibin Zheng** is a PhD student at the college of Information Engineering, Zhejiang University of Technology. He received his bachelor degree from Zhejiang University of Technology in 2017. His research interests include deep learning, artificial intelligence, and adversarial attack and defense.



**Jinyin Chen** received BS and PhD degrees from Zhejiang University of Technology, Hangzhou, China, in 2004 and 2009, respectively. She studied evolutionary computing in Ashikaga Institute of Technology, Japan in 2005 and 2006. She is currently a Professor with the Zhejiang University of Technology, Hangzhou, China. Her research interests include artificial intelligence security, graph data mining and evolutionary computing.



**Zhengguang Liu** received the the B.S. degree from Shandong University, Jinan, China, and the Ph.D. degree from Zhejiang University, Hangzhou, China, both in computer science.

He is a Postdoctoral Research Fellow with the Department of Computer Science, National University of Singapore, Singapore. His research interests include indoor localization, data mining, and intelligent systems.



**Qi Xuan** received the B.Eng. and Ph.D. degrees in control theory and engineering from Zhejiang University, Hangzhou, China, in 2003 and 2008, respectively.

He was a Post-Doctoral Researcher with the Department of Information Science and Electronic Engineering, Zhejiang University, from 2008 to 2010, and was a Research Assistant with the Department of Electronic Engineering, City University of Hong Kong, Hong Kong, in 2010. From 2012 to 2014, he was a Post-Doctoral Researcher with the Department of Computer Science, University of California at Davis, Davis, CA, USA. He is currently an Associate Professor with the College of Information Engineering, Zhejiang University of Technology, Hangzhou. His current research interests include network-based algorithm design, social network data mining, social synchronization and consensus, reaction-diffusion network dynamics, machine learning, and computer vision.



**Yue Yu** is an assistance professor in the College of Computer at National University of Defense Technology (NUDT). He received his PH.D. degree in Computer Science from NUDT in 2016. He has won Outstanding Ph.D. Thesis Award from Hunan Province. His research findings have been published on FSE, MSR, IST, ICSME, ICDM and ESEM. His current research interests include software engineering, data mining and computer-supported cooperative work.



**Yao Cheng** is currently a senior researcher at Huawei International in Singapore. She received her Ph.D. degree in Computer Science and Technology from University of Chinese Academy of Sciences. Her research interests include security and privacy in deep learning systems, block chain technology applications, Android framework vulnerability analysis, mobile application security analysis, and mobile malware detection.